PAPER • OPEN ACCESS

A numerical study on the cold sprayability of carbon fibre reinforced composites

To cite this article: A Heydari Astaraee *et al* 2023 *IOP Conf. Ser.: Mater. Sci. Eng.* **1275** 012011

IOP Conf. Series: Materials Science and Engineering 1275 (2023) 012011 doi:10.1088/1757-899X/1275/1/012011

A numerical study on the cold sprayability of carbon fibre reinforced composites

A Heydari Astaraee[1], S Bagherifard[1] and C Colombo[1]*

[1] Politecnico di Milano, Department of Mechanical Engineering, Via La Masa 1, 20156 Milano, Italy

* Corresponding author: chiara.colombo@polimi.it

Abstract. One of the open questions in cold spraying on fibre reinforced composites is the optimal thickness of the top layer to provide a suitable base for successful deposition of the metallic particles and at the same time to hinder the probable damage of the fibres. In this study, a detailed finite element model is developed to study the deformation of a single Cu particle deposition on to polyether ether ketone (PEEK) substrate reinforced with carbon fibres. A PEEK layer with 30, 40 or 60 µm thickness was considered on the top surface of the composite. The particle impact velocity was varied in the range of 300-600 m/s to analyse its effects on the induced deformations as well as the structural integrity of the critical carbon fibres. It is believed that the proposed model can provide a helpful tool for predicting the optimal conditions in the metallization of polymers using the cold spray technique.

1. Introduction

Cold gas dynamic spray or “cold spray” is a solid-state material deposition technique, where micron-sized particles of a powder bond to a substrate, as a result of the high-velocity impact and the associated severe plastic deformation. Acceleration of particles to high velocities is obtained via the expansion of a pressurized and “hot” gas through a de-Laval nozzle. Despite this, the feedstock remains in a solid state throughout the entire process; hence the name “cold” spraying.

Cold spray (CS) is primarily used to produce coatings on the surface of materials. However, it also can be adapted for repair applications and even additive manufacturing of parts [1]. The main applications deal with Metal-on-Metal coating [2], but recently attention is moving also toward Metal-on-Composites [3]. The application of CS to polymers and polymer matrix composites to produce metallic coatings is known as polymer metallization. Metallization of polymers improves their thermal and electrical properties, wear and erosion resistance, and can act as electromagnetic shielding, and as lightning strike protection for instance in the aerospace industry. Literature reports different polymer metallization methods such as metal sheet bonding, electroless plating, physical and chemical vapour deposition, and thermal spray techniques [4]. However, the metallization using CS has several advantages compared to some counterparts including: 1) reduction of processing costs, 2) possibility to get higher coating thicknesses, 3) reduction of metal oxidation, which occurs with any thermal process at high temperatures, 4) reduction of substrate degradation due to the temperature, and 4) avoid size limitations of the component, because the gun is mounted on a robot allowing for a full 3D deposition [5].

The main parameters affecting the process of coating deposition are the gas pressure, temperature and type, the powder feed rate and nozzle transverse speed, the spray distance or stand-off distance, the spray angle and the scanning step. These parameters need to be tuned properly to ensure on the one hand the cohesion between the first deposited layer and the substrate, and on the other hand the growth of the coating. In other words, there exists a valid deposition window whose selection is a challenge both from the experimental and the numerical viewpoints. Regarding the application to composites with polymeric matrix, the deposition on a thermoset matrix is extremely difficult due to erosion [6]; for this reason, most of the recent works are focusing on composites with thermoplastic matrices or including a purely thermoplastic layer at the top surface [7,8], also to prevent direct spraying over the brittle fibres. The optimal thickness of the thermoplastic top layer to provide a suitable base for a successful deposition of the metallic particles and at the same time to hinder the probable damage of the fibres is one of the open issues in cold spraying fibre reinforced composites. Indeed, limiting the mass of the overall coated structure is often a target to the designer, especially if this performing composite is applied in the aerospace field.

This strategy affects the manufacturing of the composite substrate, but definitively improves the applicability of the CS coating, especially at the first layer, where the adhesion between the polymeric substrate and the metallic coating is the weakest structural point [9]. Indeed, when dealing with the first layer (Metal-to-Composite), the particle velocity must be higher than the interlocking velocity of particles with the polymeric substrate, but lower than the erosion velocity of the polymer itself. On the other hand, dealing with the rest of the coating (Metal-to-Metal), the velocity must be higher than the critical velocity but lower than the one inducing coating erosion. For a successful deposition, the starting and key point of the coating is the first layer which is dictated by the interlocking velocity. Our previous research [10] focused on the deformation of a single Copper particle, deposited onto polyether ether ketone (PEEK). It was shown numerically that for the mechanical interlocking, a velocity threshold exists below which the particle detaches from the substrate. This numerical model predicted that the minimum particle velocity for the successful embedment and interlocking of Copper particles with 20 μm diameter in a PEEK substrate should be around 550-600 m/s, in agreement with experimental findings from the literature [11,12].

Starting from that work, we investigate here the feasibility of cold spraying Cu particles on Carbon Fibre Reinforced (CFR) PEEK with a numerical approach. A detailed finite element model is developed to study the interlocking particle velocity and to analyse the structural integrity of the fibres and the matrix. Two main manufacturing parameters are analysed with this numerical approach: the particle velocity and the thickness of the pure polymer at the impact surface. The aim is to investigate the optimal (or minimum) thickness of the PEEK layer in order to keep safe the underlying composite.

2. Numerical modelling

The three-dimensional numerical model was introduced in our previous work [10], considering the only PEEK substrate. Here, only the main points are recalled, introducing the different implementations due to the composite.

Within the FE framework of the software Abaqus/Explicit 2019, we selected a 3D Coupled Eulerian-Lagrangian formulation, widely used when dealing with high deformations as in impact problems. Here, the particle was modelled as a deformable Lagrangian section while the substrate was an Eulerian section, because of the high deformations induced during the impact. It is worth noting that generally, for Metal-to-Metal coating, the particle is simulated as Eulerian and the substrate as Lagrangian; hence, here we show a different application of these models, to the case of composites.

Figure 1.a shows the geometry as a function of the particle's radius equal to 10 μm and the boundary conditions. A friction coefficient value of 0.35 was assigned to the whole model, acting at the interface between the copper particle and the PEEK top layer. The carbon fibres were modelled explicitly as cylinders of 8 μm diameter, with a volume fraction equal to 50%. An ordered hexagonal unidirectional arrangement was considered for simplicity. The most critical fibres were those immediately below the particle. Thus, mesh size was refined only here to 1/25th of the particle's radius, to decrease the computational cost and minimize the dependency of the results on the mesh size, see Figure 1.b,c. The particle and substrate were meshed using 8-node C3D8R and EC3D8R elements with reduced

IOP Conf. Series: Materials Science and Engineering 1275 (2023) 012011 doi:10.1088/1757-899X/1275/1/012011

integration and hourglass control, respectively. Exploiting the symmetry of the problem, only a quarter of the model was built up. Thermal effects were considered using adiabatic heating conditions. A non-reflecting outflow boundary condition was applied to the bottom and side faces of the substrate, acting very similarly to infinite elements. Initial thermal boundary conditions were applied to the particles (T_p=150°C) and to the substrate (T_s=25°C).

Two input parameters were varied during the simulations, to understand their effect on the model's outputs: 1) the particles' velocity V_p, in the range 300-600 m/s, as from [10], and 2) the thickness of the PEEK layer at the top surface of the substrate, with the values 30, 40, and 60 µm taken in accordance to [7].

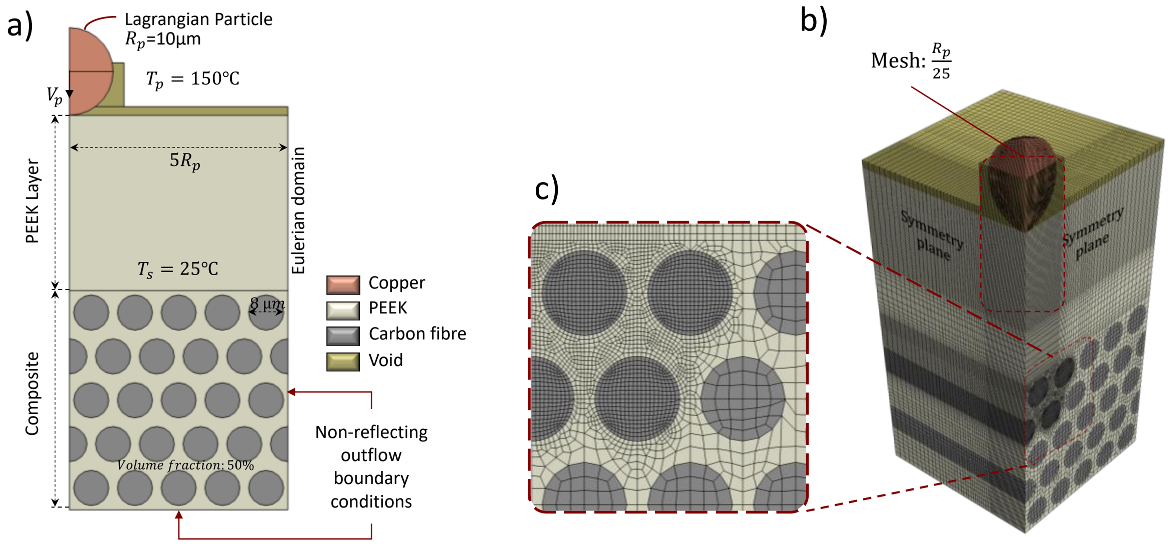

Figure 1. a) Geometry of the problem with boundary conditions; b) 3D view of the mesh and c) detail at the most refined region.

Due to the large strains, ultra-high strain rates, and thermal softening occurring during the CS, the particle and substrate materials were defined with the Johnson-Cook plasticity model [13]:

$$\sigma=\left[A+B\cdot\varepsilon_p^n\right]\left[1+C\cdot\ln\left(\frac{\dot{\varepsilon}}{\dot{\varepsilon}_0}\right)\right]\left[1-\left(\frac{T-T_0}{T_m-T_0}\right)^m\right] \quad (1)$$

where σ and ε_P are the true stress and true plastic strain, $\dot{\varepsilon}$ is the plastic strain rate, and T is the temperature variable, while A, B, n, C, m, $\dot{\varepsilon}_0$, T_0 and T_m are material constants listed in Table 1 and taken from literature works [14,15]. The constants C and m for PEEK were implemented into the software with a bilinear trend as a function of the strain rates, using the available data in the literature [16,17]. A VUHARD subroutine was used to implement this bilinear Johnson-Cook plasticity model in Abaqus. On the other hand, carbon fibres were supposed to have a linear elastic behaviour up to failure.

The use of an Eulerian domain limits high deformation of the finite elements for these cases of impact simulations. However, it is worth to point out that in this formulation, necessary for impact problems, it is not possible to include material anisotropy with the present software version.

Table 1. Material properties used in the numerical model.

Property	Copper	PEEK	Carbon Fibre
Density (kg/m^3)	8960	1300	1760
Young's modulus (GPa)	124	3.5	231
Poisson's ratio	0.34	0.40	0.28
Thermal conductivity (W/m°C)	386	0.25	8.0
Specific heat (J/kg°C)	383	Variable, see [18]	-
Elastic limit, A (MPa)	90	132	-
Hardening constant, B (MPa)	292	10	-
Hardening exponent, n	0.31	1.2	-
Strain rate constant, C	0.025	0.029 ($\dot{\varepsilon}$<100 s^{-1}) 0.0834 ($\dot{\varepsilon}\geq$100 s^{-1})	-
Reference strain rate, $\dot{\varepsilon}_0$ (s^{-1})	1.0	0.001 ($\dot{\varepsilon}$<100 s^{-1}) 1.0 ($\dot{\varepsilon}\geq$100 s^{-1})	-
Thermal exponent, m	1.09	0.634	-
Melting temperature, T_m (°C)	1083	341	-
Reference temperature, T_0 (°C)	25	23	-
Inelastic heat fraction	0.9	0.9	-

3. Results

This section presents the numerical results in terms of displacements and crater depth at the impact region, stress field in the fibres and plastic strain field in the PEEK matrix.

Figure 2.a identifies the steps during the impact of the particle over the substrate; after reaching the maximum penetration depth, when the maximum plastic strain is generated, the particle is pulled out due to the elastic reaction of the PEEK.

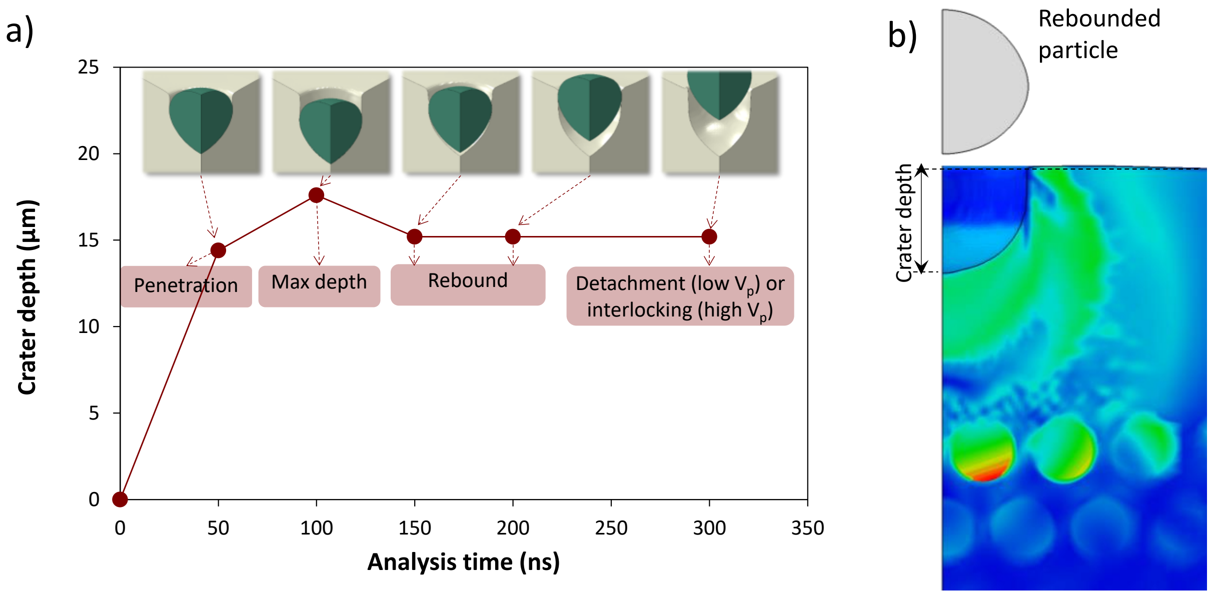

Figure 2. a) Numerical steps of the particle's impact with the corresponding trend of crater depth as a function of the numerical analysis time; b) definition of the crater depth. Images and plot refer to the impact of a Copper particle on the pure PEEK substrate, at V_p= 400 m/s; no interlocking occurs due to the low impact velocity.

Depending on the particle velocity imposed at the beginning of the simulation, the result can be the rebound with full detachment from the substrate, at $V_p < 550$ m/s, or the mechanical interlocking, at $V_p > 550$ m/s. The first result leaves an empty crater in the PEEK, resembling a hole; the second result shows a small empty region below the particle. Figure 2.b defines the crater depth as the distance between the undeformed shape and the maximum depth of the deformed shape after the elastic recovery of the PEEK, e.g., the central bottom point of the crater. The final crater depth is intended when either the particle is fully rebounded from the substrate (if the velocity is not sufficient for the embedment) or stays embedded (if the particle velocity is sufficiently high to reach mechanical interlocking). All the simulations clearly show the indentation, and the penetration depth is always not null.

Figure 3 summarizes the numerical results of the crater depth as a function of V_p and PEEK thickness at the top of the CFR polymer. The figure also shows the interlocking limit identified from the analyses.

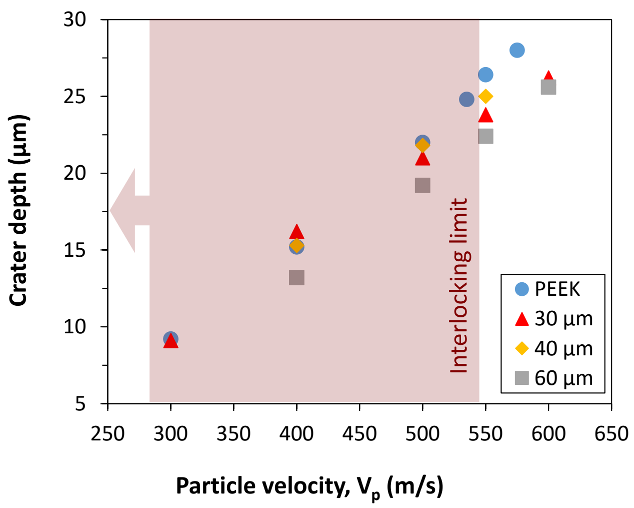

Figure 3. Trend of the crater depth as a function of the particle impact velocity; comparison between the case of pure PEEK substrate and the cases of a PEEK layer with different thicknesses at the top of the CFR polymer.

Before analysing the output of the model in terms of stress and strains, Figure 4 compares the peak stress in the fibres with two formulations, i.e., the coupled Eulerian-Lagrangian (CEL) model, described previously in Section 2, and the purely Lagrangian model with infinite boundary conditions. Indeed, literature reports that the nodal stress/strains of the Eulerian domain are not realistic, because the material flows through the mesh, fixed in the space [19]. Instead, it is suggested to use the volume-averaged variables. This direct comparison between the two models ensures that the averaged stresses are providing realistic values. The comparison is performed at the low velocity of 400 m/s, since the Lagrangian analysis does not abort, even if extremely distorted elements with a non-favourable aspect ratio in the crater can be observed in Figure 4.c. Figure 4.a shows that the averaged von Mises stress in the Eulerian model is very similar to the nodal von Mises stress in the Lagrangian model, suggesting the validity of the volume-averaged stress. The difference after the peak point in Figure 4.a between the two trends (CEL vs. L models) as a function of time could be attributed to the extremely distorted mesh of the Lagrangian model which deteriorates the results.

Once the validity of the outputs is confirmed, Figure 5 and Figure 6 show the stress and the equivalent plastic strain fields, respectively. Both these quantities are averaged volume over the finite element volume (SVAVG is the volume-averaged von Mises stress and PEEQAVG is the equivalent volume-averaged plastic strain). The most stressed region is the fibre placed below the impact (Figure 5.a), while the most strained one is the matrix at the crater, together with some intensification occurring in the region of the most stressed fibre (Figure 6.a,b).

IOP Conf. Series: Materials Science and Engineering 1275 (2023) 012011 doi:10.1088/1757-899X/1275/1/012011

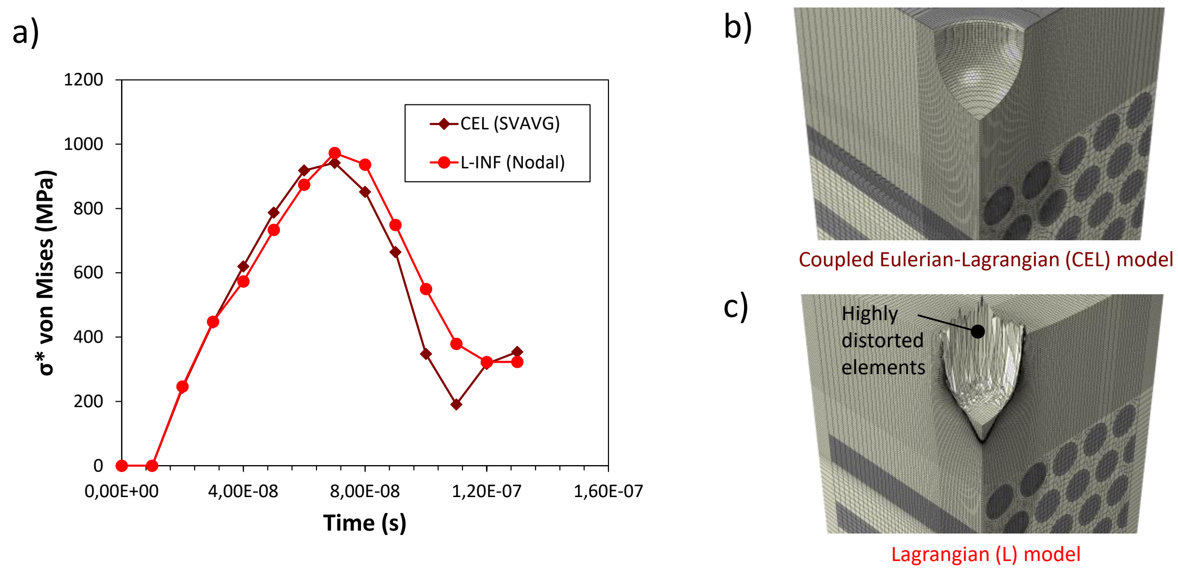

Figure 4. a) Trend of the equivalent von Mises stress at the most stressed carbon fibre as a function of the analysis time: comparison between a Coupled Eulerian-Lagrangian (CEL) model and a Lagrangian (L) model; b) CEL deformed shape and c) L deformed shape. Impact particle velocity: $V_p = 400$ m/s.

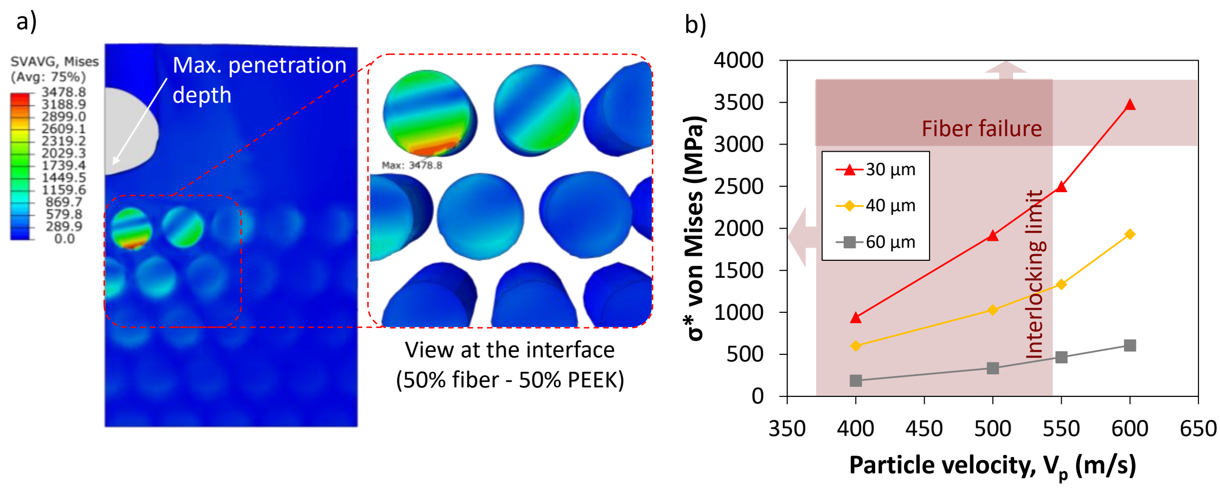

Figure 5. Numerical results into the fibres: a) von Mises equivalent stress field averaged over the element's volume (SVAVG), with a detail at the fibre region, for the case of a surface PEEK layer with 30 μm thickness and $V_p = 600$ m/s; b) trend of the maximum von Mises stress as a function of the particle velocity.

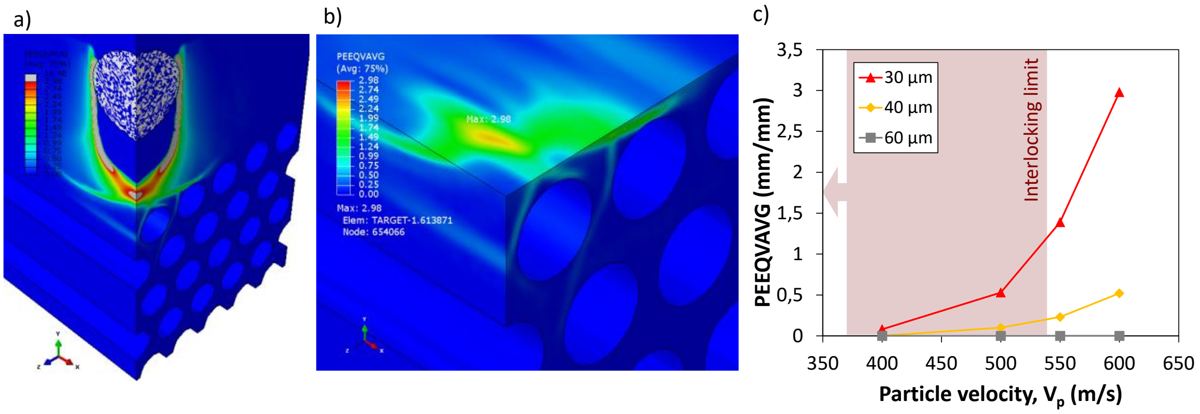

Figure 6. Numerical results in the PEEK: a) equivalent plastic strain field averaged over the element's volume (PEEQAVG), for the case of a surface PEEK layer with 30 μm thickness and V_p = 600 m/s; b) detail at the interface between the pure PEEK and the composite; c) trend of the maximum value of the PEEQAVG in the PEEK as a function of the particle velocity.

After showing these outputs of the simulation, the model was modified to study the dependence of the SVAVG in the fibres and of the PEEQAVG in the matrix as a function of the distance between the fibres, e.g. of the local fibre volume, that can locally increase also due to the randomness of the fibre positioning. Figure 7 shows the plots for the case of a pure polymeric layer with 30 μm thickness. Here, the results of inter-distance equal to 3 μm (solid line) correspond to the previous simulations, while a second case with 0.5 μm inter-distance (dashed line) is added as a comparison, showing the trend of stresses and strains in the substrate.

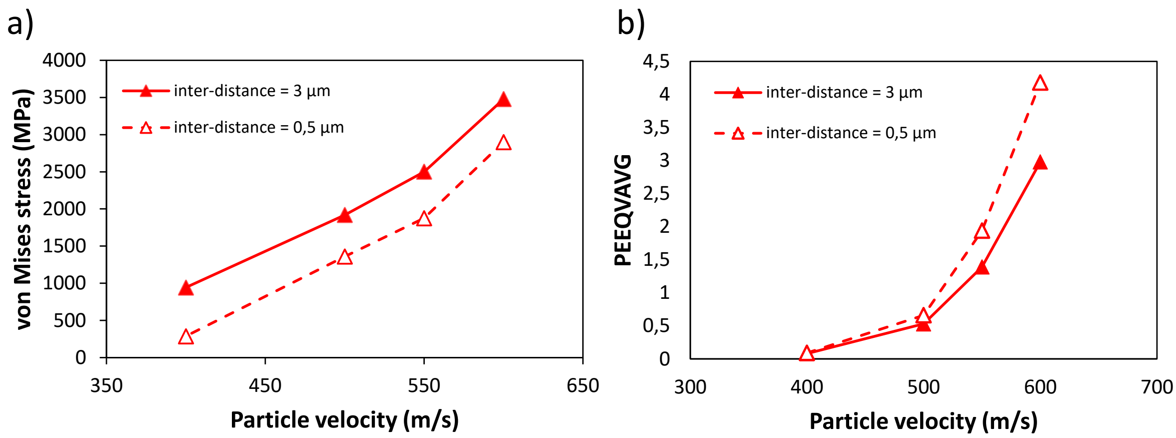

Figure 7. Effect of the distance between the fibres on: a) SVAVG in the fibres; b) PEEQAVG in the matrix. Case of 30 μm thickness, with variable particle velocity.

4. Discussion

Different interesting outputs can be obtained from the implemented numerical models, which are worth discussing with some focus on the impact region as well as at the composite level.

Focusing at first on the crater depth, Figure 3 shows linear trends in the investigated range of vertical particle velocities, both for pure PEEK as well as for PEEK with a composite substrate. The crater depths are lower for the cases with a composite substrate compared to the pure PEEK substrate, meaning that the underlying composite increases the stiffness of the structure and offers resistance to deformation. However, the model is not very sensitive to the underlying composite. Indeed, the difference can be appreciated only at sufficiently high particle velocities. In these cases, the difference is less than 20% with respect to the case of pure PEEK substrate. Figure 3 also reports the interlocking limit of 550 m/s, which is insensitive to the presence of the CFR region below the PEEK. Providing that this layer is placed at the surface, the models always identified the interlocking phenomenon occurring at the same velocity.

It is worth noting that the crater depth, which is an indicator of the coating penetration into the substrate, suggests the required minimum thickness of the PEEK bond layer to serve as protection for the fibres. In other words, the minimum PEEK thickness could not be lower than the final crater depth. This structural condition is necessary but not sufficient because also the failure of the fibres or the PEEK matrix can occur. For this reason, it is important to focus also on stresses and strains below the impact region.

Focusing on the fibres, the maximum equivalent stress is always in the fibre immediately below the impact region, with a gradient due to the induced bending (Figure 5.a), e.g., the most stressed area of the fibre is in its south pole region. Besides, the time interval when maximum stress occurs is close to the maximum penetration of the particle in the PEEK matrix. Although the other fibres are also stressed, the stress level decreases with increasing distance from the point of impact. The plot of Figure 5.b summarizes the results from the simulations of the single particle impact with different PEEK thicknesses. As expected, the maximum stress increases with a decrease in the thickness. However, the stress growth is more considerable at higher particle velocities, experiencing a nonlinear trend. Here, a successful window of deposition is identified, dictated by two conditions: 1) the upper limit of carbon fibre strength that is around 3000 MPa [20], and 2) the effective interlocking of the particle, generating the first layer, as seen in Figure 3. Figure 5.b suggests that a PEEK layer of 60 μm is a good choice because the developed stresses remain well below the fracture strength of the fibres even upon high velocities, while 30 μm thickness is too small to ensure a good safety factor in the fibres, especially at the velocities allowing for the interlocking.

On the other hand, it is necessary to examine also the PEEK matrix in terms of volume-averaged equivalent plastic strain (PEEQAVG). This field underlines some cruciality at the most critical fibres, acting as a strain raiser (Figure 6.a,b). It was found that the only region experiencing plasticity is above the most critical fibre. Besides, it should be noted that the highest PEEQAVG value (3 mm/mm) is due to the severe plasticity around the crater, which is not structurally interesting for the composite. Figure 6.c summarizes the peak PEEQAVG in the matrix at the fibre region. It is difficult to add a limitation in this plot because the strain limit depends on the triaxiality, which is not an available output of the simulation. However, it is clear that with 60 μm thickness no failure will occur.

Since the PEEQAVG are null for such a layer thickness, the case with 30 μm of pure PEEK as the top layer was selected to understand the effect of the different inter-fibre distance on the stresses in the fibres and strains in the matrix. Figure 7 gives a comparative trend and underlines that there is an almost constant difference in the peak stress values of about 600 MPa (Figure 7.a), while strains in the matrix progressively increase with the particle velocity reaching +40% at 600 m/s (Figure 7.b). Even if these strain values could be beyond the limit of the PEEK, the model can catch the effect of this parameter, underlying the weakest regions more prone to the failure.

All these numerical results agree with the experimental work by Gillet et al. [7], suggesting that in the case of cold sprayed Copper coating over a carbon reinforced composite, it is necessary to place a pure PEEK top layer with a thickness in the range of 50-100 μm. This direct comparison underlines the importance of numerical models in the selection of the optimal manufacturing strategies for such new coatings. Indeed, cold spray is a recent technology recently spreading; the implementation and validation of a numerical model can be extremely useful to save time and costs for experimental campaigns and allow for a quick selection of targeted experiments.

5. Conclusion

The implemented numerical model of a single Copper particle impact on a substrate made of a top layer of pure PEEK and an underlying carbon fibre reinforced composite was in good agreement with experimental literature data. For all the cold spray parameters set in this study, a 60 μm PEEK bond layer was found to be safe while a 30 μm is not recommended.

From a more general viewpoint, the model can:

- estimate the interlocking velocity of the particle in the PEEK layer, suggesting that the minimum PEEK thickness could not be lower than the final crater depth;
- evaluate the maximum stress in the most critical fibre;
- evaluate the maximum equivalent plastic strain in the matrix.

These three conditions identify structural limits to the mechanical resistance of the coated composite. As an application of this model, the effect of a change in the inter-fibre distance was analysed, showing the trends of stresses in the fibres and strains in the matrix. Future steps of the work will consider different distributions and arrangements of the fibres as well as study the effect of a multiple impact.

From a wider perspective, this numerical approach could be a valid tool to select the best deposition window during cold spray manufacturing, performing targeted experiments.

Acknowledgements

This research is part of the project COSMEC (Cold Spray of Metal to Composite), funded by the Italian Ministry of University and Research (MUR) under the call PRIN2017 (Grant 2017N4422T).

References

[1] Yin S, Cavaliere P, Aldwell B, Jenkins R, Liao H, Li W and Lupoi R 2018 Cold spray additive manufacturing and repair: Fundamentals and applications *Addit. Manuf.* **21** 628–50
[2] Prashar G and Vasudev H 2021 A comprehensive review on sustainable cold spray additive manufacturing: State of the art, challenges and future challenges *J. Clean. Prod.* **310**
[3] Sandhu H S, Phull G S, Anand U, Preet Singh J and Gulati P 2021 Deposition of Metallic Coating on Plastic Substrate Material Using Cold Spray *Lect. Notes Mech. Eng.* 61–70
[4] Melentiev R, Yudhanto A, Tao R, Vuchkov T and Lubineau G 2022 Metallization of polymers and composites: State-of-the-art approaches *Mater. Des.* **221**
[5] Parmar H, Tucci F, Carlone P and Sudarshan T S 2022 Metallisation of polymers and polymer matrix composites by cold spray: state of the art and research perspectives *Int. Mater. Rev.* **67** 385–409
[6] Che H, Chu X, Vo P and Yue S 2017 Cold spray of mixed metal powders on carbon fibre reinforced polymers *Surf. Coatings Technol.* **329** 232–43
[7] Gillet V, Aubignat E, Costil S, Courant B, Langlade C, Casari P, Knapp W and Planche M P 2019 Development of low pressure cold sprayed copper coatings on carbon fiber reinforced polymer (CFRP) *Surf. Coatings Technol.* **364** 306–16
[8] Astaraee A H, Salerno A, Bagherifard S, Carlone P, Parmar H, Astarita A, Viscusi A and Colombo C 2021 Thermographic analysis of composite metallization through cold spray *Metals (Basel).* **11**
[9] Raoelison R N, Lalu Koithara L and Costil S 2021 Cold spray coating of PEEK surface by copper deposition: Interfacial adhesion at high deposition efficiency and bonding strength *CIRP J. Manuf. Sci. Technol.* **35** 63–8
[10] Heydari Astaraee A, Colombo C and Bagherifard S 2021 Numerical Modeling of Bond Formation in Polymer Surface Metallization Using Cold Spray *J. Therm. Spray Technol.*
[11] Bortolussi V 2016 *Experimental and Numerical Study of the Electrical Conductivity of Cold Spray Metal-Polymer Composite Coatings on Carbon Fiber-Reinforced Polymer* (Université Paris sciences et lettres)
[12] Che H, Vo P and Yue S 2019 Investigation of Cold Spray on Polymers by Single Particle Impact Experiments *J. Therm. Spray Technol.* **28** 135–43

[13] Johnson, R. G 1983 A constitutive model and data for materials subjected to large strains, high strain rates, and high temperatures *Proc. 7th Inf. Sympo. Ballist.* 541–7

[14] Wang Q, Luo X, Tsutsumi S, Sasaki T, Li C and Ma N 2020 Measurement and analysis of cold spray residual stress using arbitrary Lagrangian–Eulerian method *Addit. Manuf.* **35**

[15] Garcia-Gonzalez D, Rusinek A, Jankowiak T and Arias A 2015 Mechanical impact behavior of polyether-ether-ketone (PEEK) *Compos. Struct.* **124** 88–99

[16] Rae P J, Brown E N and Orler E B 2007 The mechanical properties of poly(ether-ether-ketone) (PEEK) with emphasis on the large compressive strain response *Polymer (Guildf).* **48** 598–615

[17] El-Qoubaa Z and Othman R 2017 Temperature, Strain Rate and Pressure Sensitivity of the Polyetheretherketone's Yield Stress *Int. J. Appl. Mech.* **9**

[18] Koerdt M, Koerdt M, Grobrüg T, Skowronek M and Herrmann A S 2022 Modelling and analysis of the thermal characteristic of thermoplastic composites from hybrid textiles during compression moulding *J. Thermoplast. Compos. Mater.* **35** 127–46

[19] Oyinbo S T and Jen T C 2020 Feasibility of numerical simulation methods on the Cold Gas Dynamic Spray (CGDS) Deposition process for ductile materials *Manuf. Rev.* **7**

[20] Minus M L and Kumar S 2005 The processing, properties, and structure of carbon fibers *Jom* **57** 52–8